

## Article

# Designing Sustainable Ethanol Oxidation Catalysts: The Role of Graphene Oxide in NiCuGO Composite Material

Marta Wala-Kapica, Magdalena Szewczyk and Wojciech Simka \* 

Department of Inorganic Chemistry, Analytical Chemistry and Electrochemistry, Faculty of Chemistry, Silesian University of Technology, 44-100 Gliwice, Poland; marta.wala-kapica@polsl.pl (M.W.-K.); magdsze594@student.polsl.pl (M.S.)

\* Correspondence: wojciech.simka@polsl.pl

**Abstract:** The growing world population with the growth of civilization is causing the demand for electric energy to increase every year. For this reason, new energy sources such as fuel cells are becoming more and more needed, especially when they can use renewable fuel such as ethanol. This simple organic alcohol can be easily produced in a fermentation process using organic waste. Its oxidation might be used as a source for electricity; however, due to the lack of proper electrocatalytic materials, such a solution is not popular. A simple method of NiCuGO composite preparation via electrodeposition from a water-based solution containing graphene oxide suspension is proposed. The activity of the prepared material is proven, with higher current densities observed for the composite powder. The highest peak current density is observed for NiCuGO deposited with a higher current density. The observed  $i_{pA}$  of  $8.6 \text{ mA cm}^{-2}$  has been higher than that reported by other researchers.

**Keywords:** ethanol oxidation; fuel cell; nickel; copper; graphene oxide; composite; electrodeposition



**Citation:** Wala-Kapica, M.; Szewczyk, M.; Simka, W. Designing Sustainable Ethanol Oxidation Catalysts: The Role of Graphene Oxide in NiCuGO Composite Material. *Energies* **2024**, *17*, 288. <https://doi.org/10.3390/en17020288>

Academic Editor: Renato Somma

Received: 31 October 2023

Revised: 26 November 2023

Accepted: 3 January 2024

Published: 5 January 2024



**Copyright:** © 2024 by the authors. Licensee MDPI, Basel, Switzerland. This article is an open access article distributed under the terms and conditions of the Creative Commons Attribution (CC BY) license (<https://creativecommons.org/licenses/by/4.0/>).

## 1. Introduction

Fuel cells stand as a leading contender in the quest for green energy solutions, offering high efficiency and a low environmental impact. However, the widespread adoption of fuel cells is hindered by the limited performance and high cost of materials employed in their construction, particularly within the anodic components [1–3]. The continuous pursuit of alternative materials that can enhance the efficiency, stability, and cost-effectiveness of fuel cells has led to the exploration of various composite materials [1,3].

Simple alcohols have increasingly received attention as potential fuel sources due to their practicality as energy providers. Their attraction primarily lies in their high energy densities, low toxicity, and ease of both storage and transportation. Among these alcohols, ethanol stands out prominently due to its remarkable suitability arising from the straightforward synthesis via the biological process of fermentation. This unique characteristic endows ethanol with a renewable nature. Notably, virtually any organic source, especially one abundant in carbohydrates, can be utilized as feedstock for ethanol production, reinforcing its renewable quality. This inherent characteristic underscores the potential for an eco-friendly and sustainable energy source, fostering continued interest and exploration in alcohols as a viable fuel alternative [3–7].

Among the multitude of materials under investigation, nickel and copper emerge as promising candidates due to their catalytic properties and abundance [8–14]. Additionally, the integration of graphene oxide—a remarkable two-dimensional carbon-based material known for its exceptional conductivity, and large surface area—presents an exciting avenue for enhancing the performance of fuel cell components [13,15–20].

Nickel-based materials have been proven to be active towards ethanol oxidation. The synergic effect of its mixing with copper has also been reported to be beneficial for

hydrogen evolution [21,22], oxygen evolution [23], oxygen reduction [24], methanol oxidation [25], urea oxidation, [26,27] ethanol oxidation [28] and dehydrogenation [29,30]. The amalgamation of these materials aims to leverage the synergistic effects of their individual properties, capitalizing on the catalytic activity of nickel and copper while harnessing the conductivity and structural reinforcement provided by graphene oxide. The addition of copper to Ni-based catalysts has been proven to increase its activity due to the electronic effect, which is related to the vacancy in the filling of the *d* band of nickel and in the suppression of the formation of less active  $\gamma$ -NiOOH [31,32]. Another explanation of the higher activity of Ni catalysts doped with Cu is a bifunctional mechanism, where the Cu atoms are active centers for OH<sup>-</sup> ion adsorption [29,33] and increased immunity toward CO poisoning caused by the presence of Cu [27]. Such activity could be even further increased via the preparation of composite material, consisting of both Ni and Cu metals with the addition of carbon nanomaterial, which would not only improve the conductivity of the final material, but also increase its active surface area and the particles' dispersion during electrodeposition [15,34–41].

This article presents a comprehensive study detailing the synthesis and characterization of a new composite material consisting of nickel, copper, and graphene oxide for ethanol fuel cell anodes. The NiCuGO composite prepared via the electrodeposition of a water suspension, which has been shown to be active towards methanol [42] and urea [43], is now examined for ethanol oxidation. The addition of graphene oxide has been proven to increase the surface area of the proposed material and increase its activity toward methanol and urea oxidation. Since ethanol is a much more complicated particle and the breaking of the strong intercarbon bond is not easy, this article focusses on an examination of the activity of the proposed material towards its oxidation and the role of graphene oxide in the process.

The proposed material was synthesized via electrodeposition from a water-based electrolytic bath, offering a streamlined, rapid, and environmentally friendly process. This methodology stands out for its exclusion of toxic organic substances, such as hydrazine or NH<sub>4</sub>F, commonly employed in the synthesis of similar materials [35,44–47]. Moreover, the electrodeposition process provides a versatile means to tailor the final material by adjusting various process parameters, including current density and electrolyte composition [41,48–51]. This adaptability allows for precise control over the material's characteristics, demonstrating a flexible and efficient approach to material design and synthesis.

The best results were observed for a NiCuGO composite electrodeposited with a current density of 20.8 A dm<sup>-2</sup>. The peak current density for ethanol oxidation was 8.6 mA cm<sup>-2</sup> at a peak potential of 0.66 V vs. Ag | AgCl<sub>(sat.KCl)</sub> and 9.1 mA cm<sup>-2</sup> at a peak potential of 0.7 V vs. Ag | AgCl<sub>(sat.KCl)</sub>.

## 2. Materials and Methods

All used chemicals were of analytical purity, and were manufactured by Avantor (Gliwice, Poland).

The proposed method of composite powder preparation has been described elsewhere [42]. Briefly, to a water-based solution containing nickel and copper salts with the addition of citric acid as a complexing agent suspension, 0.5 g L<sup>-1</sup> of graphene oxide (Graphene Supermarket, Ronkonkoma, NY, USA) was added. Using the power source with a current density of 15.6 A dm<sup>-2</sup> and 20.8 A dm<sup>-2</sup> working in constant-current mode for 10 and 5 min, respectively, the proposed materials were electrodeposited in the forms of powders, which were taken off the base metal using ultrasounds, dried and cleaned. Depending on the used current density and the electrolyte ingredients, samples were named, as shown in Table 1.

**Table 1.** Clarification of samples codes used further in the text.

Sample Name	GO Addition, g L <sup>-1</sup>	<i>i</i> , A dm <sup>-2</sup>
NiCu15	-	15.6
NiCu20	-	20.8
NiCuGO15	0.5	15.6
NiCuGO20	0.5	20.8

The electrochemical activity of prepared materials was assessed using the AUTOLAB PGSTAT302N potentiostat with NOVA 2.1 software (Metrohm, Herisau, Switzerland). For electrochemical measurements, a three-electrode system was used, with glassy carbon as a counter electrode and Ag | AgCl<sub>(sat.KCl)</sub> as a reference electrode, which is why all the potentials mentioned in this paper will be given in the reference to this electrode.

All mentioned measurements were made on stationary working electrodes, which were prepared via the deposition of 5 µL of catalytic ink on a polished glassy carbon electrode (ϕ 5 mm). Catalytic ink was prepared by mixing the prepared powder (1 mg of powder per 30 µL of ink) with Nafion<sup>®</sup> and Isopropanol solutions (1:10 *v/v*), followed by ultrasound mixing until deep black catalytic ink was prepared.

The activity of the proposed material was examined using cyclic voltammetry in the voltage range of 0–0.7 V vs. Ag | AgCl<sub>(sat.KCl)</sub>, linear sweep voltammetry and chronoamperometry.

The best activity of the proposed powders was observed in 1 M KOH, which was used as a supporting electrolyte for ethanol. The concentration of ethanol was experimentally chosen via a series of CV experiments in solutions with various (1–5 M) ethanol concentrations.

Scanning electron microscopy (SEM) was conducted using Hitachi S-4000N (Hitachi, Tokyo, Japan) with an exceeding voltage of 15 kV. Based on SEM images, particle size analysis was conducted using the ImageJ 1.5 (NIH, Bethesda, MD, USA) graphical software. The size of the particle edges was measured at 50 points for each modification.

### 3. Results and Discussion

The proposed powders were examined using XRD [42], XPS and Raman methods [43]. They were proven to be Cu<sub>0.21</sub>Ni<sub>0.79</sub> alloys with the presence of GO. On the surface, powders were covered with metal oxides or salts.

The morphology of obtained powders was typical for metallic powders electrodeposited with a high current density. Dendrite- or coral-like particles were formed due to the electrodeposition process taking place at the same time with hydrogen evolution. Gas bubbles forming on the surface of the substrate played the role of a dynamic template, which leading to the highly developed surface with a highly electroactive surface [52–55]. Such a quality is very beneficial for the potential use of electrodeposits as catalysts, since this process has a strong surface characteristic, and its yield is strictly related to the size of the electroactive surface. The dendritic morphology of catalyst is related to the strengthened electric field distribution, which prompts local OH<sup>-</sup> enrichment in the electrical double layer (EDL), so the catalytic effect of the material is reinforced [56].

The morphology of the prepared working electrode is shown in Figure 1.

Based on the SEM images of proposed samples, the distribution of particles size was evaluated (Figure 2). From these plots, we can conclude that the usage of a higher current density leads to the electrodeposition of smaller particles, which suggests that the speed of nucleus formation is higher than the speed of nucleus propagation.

Interestingly, the addition of graphene oxide into the electrolyte led to the formation of smaller particles, despite the use of a smaller current density, which suggests that the presence of GO in the electrolytic bath changed the deposition mechanism more strongly than just its incorporation into the final material. The smallest particles were observed for NiCuGO20 powder, which suggests that this powder should have the highest electroactive surface (ECSA), which has been already proven [42]. Its superior activity has already been proven for 1 M KOH solution with and without the addition of methanol and urea.

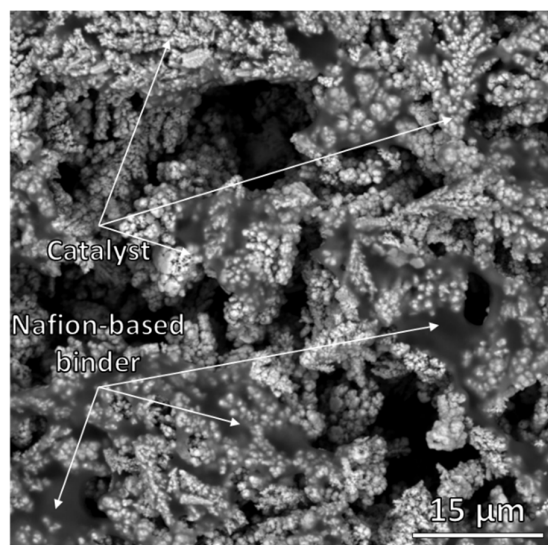


**Figure 1.** SEM image of NiCuGO20-based working electrode.

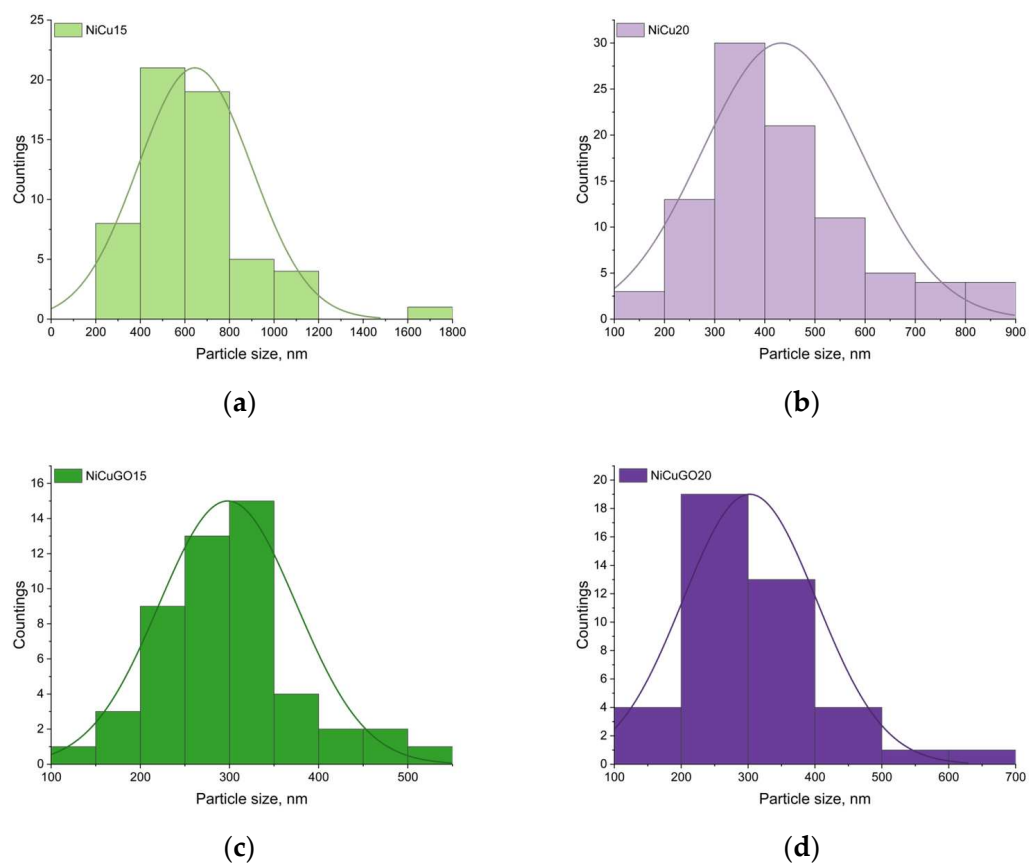


**Figure 2.** Particle size distribution of prepared materials: (a) NiCu15, (b) NiCu20, (c) NiCuGO15 and (d) NiCuGO20.

### 3.1. Influence of Ethanol Concentrations

Prior to investigating the electrochemical activity of the proposed materials for ethanol oxidation, we conducted preliminary assessments of their performance in various KOH solutions to determine the optimal electrolyte concentration. Figure 3 illustrates the representative current response recorded for NiCuGO20. As the KOH concentration increased from 0.5 to 1 M, there was a noticeable rise in the peak current density. However, it is noteworthy that a further increase in KOH concentration from 1 to 2 M did not result

in a corresponding increase in current density. On the contrary, the observed peak was smaller than that recorded in the 1 M solution. Since this trend was consistent across all prepared powders, we selected a 1 M KOH concentration as the supporting electrolyte for subsequent studies.

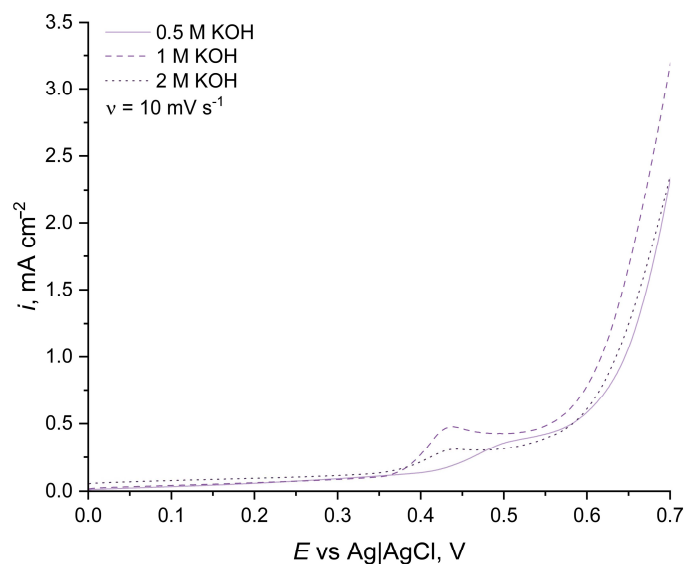


**Figure 3.** Linear sweep voltammetry results for NiCuGO20 powder.

### 3.2. Activity towards Ethanol Oxidation

The assessment of proposed material activity started with an investigation of the influence of ethanol concentration on the activity of the proposed materials.

The ethanol concentration for further electroactivity studies was chosen based on a series of voltametric experiments. Briefly, 1 M KOH solutions with the addition of 1, 2 and 5 M of ethanol were prepared, and the activity of the proposed samples were examined, as presented in Figure 4.

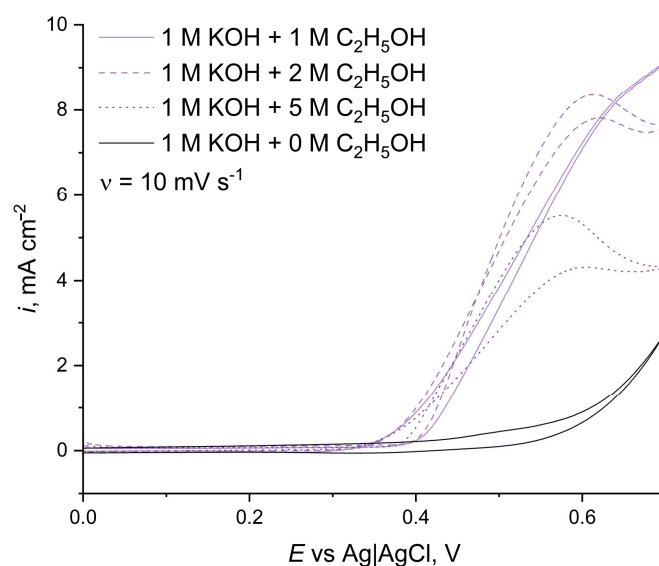


**Figure 4.** Cyclic voltammograms of NiCuGO20 powder in 1 M KOH with the addition of various ethanol concentrations.

The highest current density was observed for 1 M ethanol solution. A lower concentration of this alcohol resulted in lower peak current densities, and interestingly, a further increase also led to lower peak current densities, which was probably related to the usage of all active centers by 1 M of this molecule.

### 3.3. Activity towards Ethanol Oxidation

All the proposed powders showed activity towards ethanol oxidation, as shown in Figure 5. During the forwards scan, an oxidation peak was visible, which was related to the reactions [13,57–59]:

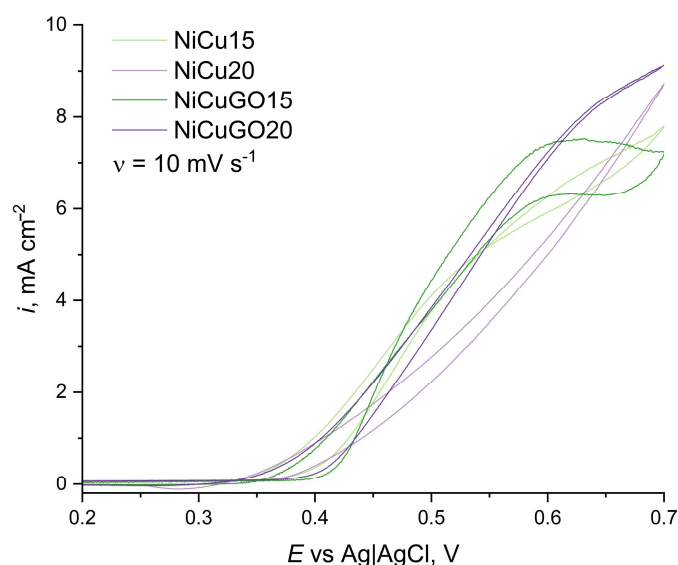
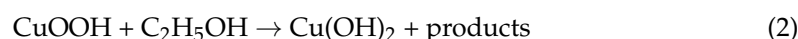
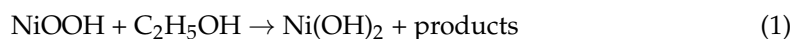


Figure 5. Cyclic voltammogram of prepared powders; 1 M KOH + 1 M ethanol.

Unfortunately, we cannot conclude what the products of such a reaction are. Ethanol oxidation can take place via two different mechanisms: C1, leading to  $\text{CO}_2$  as a reaction product, or the C2 pathway, leading mostly to acetic acid and acetaldehyde [60,61]. We have not examined volatile or liquid products in the reaction mixture, which is why no further conclusions can be considered and why further studies of the GO influence on the materials' activity are needed.

Powder NiCu20 has shown slightly different behavior compared to that of the other examined materials, since in its voltammograms no clear oxidation peak was visible. Such a difference might be related to the different mechanisms of ethanol oxidation and thus the lack of a stable diffusion layer causing the characteristic CV shape for oxidation reactions.

Nevertheless, we can conclude that its activity towards ethanol oxidation is lower than its composite equivalent, since its current outcomes were lower in the whole voltage range in which the CV scans were conducted.

The highest activity, proven by the highest peak current density, with a value of  $8.6 \text{ mA cm}^{-2}$ , was observed for NiCuGO20 composite powder. Interestingly, the peak current density observed for NiCuGO15 composite is lower than the one observed for its alloy equivalent (see Table 2). Such a difference shows once again that the mechanism of the influence of graphene oxide on material activity is not so easy to determine, and that other parameters, such as the mean particle size, related to the deposition current density, can change the final material's activity even more strongly than can just the presence of graphene oxide.

**Table 2.** Comparison of observed current outcomes at oxidation peaks and at reverse potential (0.7 V vs. Ag | AgCl<sub>(sat.KCl)</sub>).

Sample	$E_{pA}$ , V	$i_{pA}$ , mA cm <sup>-2</sup>	$i_{@Erev}$ , mA cm <sup>-2</sup>
NiCu15	0.65	7.05	7.75
NiCu20	-	-	8.70
NiCuGO15	0.63	7.5	7.25
NiCuGO20	0.66	8.6	9.10

$E_{pA}$ —anodic peak potential;  $i_{pA}$ —anodic peak current density;  $i_{@Erev}$ —peak current density at the reverse potential.

Similar materials described in the literature have shown lower peak current densities, from 4.03 mA cm<sup>-2</sup> observed for nanomaterial Ni<sub>20</sub>@Pd<sub>60</sub>Rh<sub>20</sub> [62] through to 5.6 mA cm<sup>-2</sup> for Ni-doped platinum [63]. As it is presented in Table 3 below, similar activity has been reported for electrodeposited NiCu material, with an  $i_{pA}$  of 12.4 mA cm<sup>-2</sup> [64]. Ni-Co composite deposited on reduced, nitrogen-doped GO has shown even higher activity, this being 64.2 mA cm<sup>-2</sup> [65]. For NiCu nanorods, the recorded peak current density was 86.1 mA cm<sup>-2</sup> [58]. A catalyst based on Ni, Cu and Fe<sub>2</sub>O<sub>3</sub> showed even higher activity with an  $i_{pA}$  of 101 mA cm<sup>-2</sup> [66], similarly to mixed a Ni-NiO catalyst, which had a peak current density of 120 mA cm<sup>-2</sup> [67]. Catalysts consisting of Pd doped with Cu [68] or Cd with the addition of reduced GO [69] have shown an  $i_{pA}$  of 166 and 179 mA cm<sup>-2</sup>, respectively. Other dopants used for Ni-based catalysts, such as Co or Cr<sub>2</sub>O<sub>3</sub>, have also led to an increase in the recorded peak current density up to 181 [57] and 327 mA cm<sup>-2</sup> [70], respectively.

**Table 3.** Comparison of the proposed materials with the materials described in the literature.

Material	$i_{pA}$ , mA cm <sup>-2</sup>	Reference
NiCuGO20	8.6	This article
NiCo	180	[57]
NiCu NR	86.1	[58]
Ni <sub>20</sub> @Pd <sub>60</sub> Rh <sub>20</sub> /C	4.0	[62]
PtNi/C	5.6	[63]
NiCu	12.4	[64]
NiCo@ErN-GO	64.2	[65]
NiCuFe <sub>2</sub> O <sub>3</sub>	101	[66]
Ni-NiO	120	[67]
PdCu	166	[68]
PdCdrGO	179	[69]
Ni-Cr <sub>2</sub> O <sub>3</sub>	327	[70]

NR—nanorods.

The proposed composite showed higher activity than that of nickel-based nanomaterials. However, it showed lower activity than that of a similar NiCu-based material, which was probably caused by the bigger size of the prepared particles, leading to a lower active surface. Despite the lower activity, the proposed catalyst can still be a good candidate as an ethanol oxidation catalyst due to its rapid synthesis and stability.

### 3.4. Stability during Ethanol Oxidation

As presented in Figure 6, all proposed materials were proven to be stable during 1800 s polarization to their peak potential. After the start of polarization, initially, the current density grew, contrastingly to the usually recorded drop related to the charging of the dielectric layer. In this case, the current response grew, which has also been reported for similar materials [71].

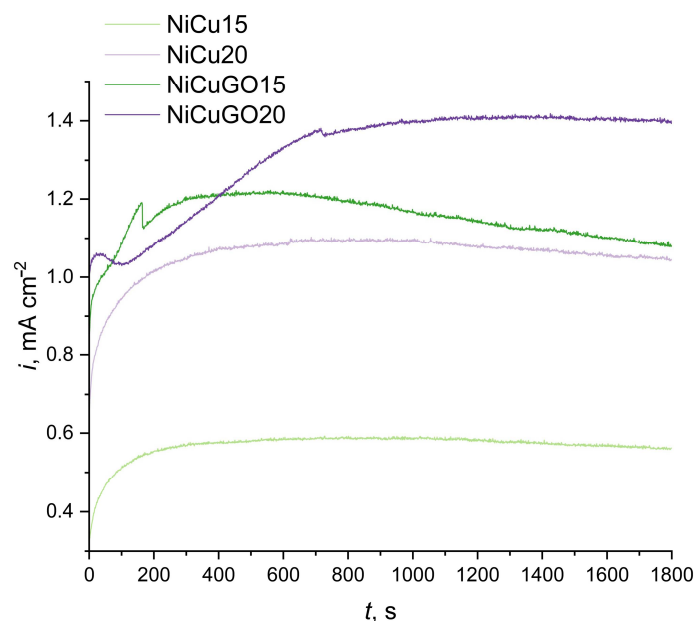


**Figure 6.** Results of chronoamperometric studies recorded for 1800 s at the anodic peak potential.

Such behavior is related to the fact that ethanol as an organic molecule consisting of two carbon atoms is not easy to be fully oxidized. The quality that makes it such a stable compound, making it a perfect fuel to store and transport, also makes it hard to fully oxidize. The stable bond between the two carbon atoms is very hard to break, which is why ethanol oxidation might need more time and would explain why after the beginning of polarization to the peak potential current the response grows with time until it stabilizes. The peak visible on the CA curves is probably related to the moment when the multistep ethanol oxidation reaction would have occurred with the highest efficiency. The lowering of current densities recorded at the peak potential might be related to the slight poisoning of the catalyst from the reaction products or to the mechanical detachment of the catalyst caused by the gaseous products' evolution. Once again, the highest activity was observed for NiCuGO20 composite, which proves that this modification is not only the most active during voltametric studies, but also that it preserves its activity during long-term examination.

The ethanol oxidation mechanism on NiCuGO composite catalysts is a complex process that involves multiple steps, with a key focus on the regeneration of active sites [72,73]. Notably, other researchers have emphasized that the activity of the system can be significantly enhanced through the incorporation of certain agents that improve electron conductivity [66,74,75]. The NiCuGO composite catalyst appears to benefit from the addition of graphene oxide, which plays a crucial role in facilitating electron transfer during the ethanol oxidation process. The high electron conductivity of GO contributes to the overall efficiency of the catalyst, making it a promising material for ethanol oxidation applications.

#### 4. Conclusions

In the presented paper, a quick and easy method of electrocatalyst composite preparation is described. The properties of the final material can be tailored by changing the conditions of the electrodeposition process, which is a huge advantage of the proposed method. It has been proven that the addition of graphene oxide into the electrolytic bath strongly influences the properties of the final material, leading to its smaller particle sizes and higher activity. The best results in terms of ethanol oxidation were observed for NiCuGO20 composite, which shows that there is a strong correlation between the process parameters and the properties of the prepared material. Higher deposition current densities and the presence of GO in the electrolytic bath lead to the formation of more active particles.

**Author Contributions:** Conceptualization, M.W.-K. and W.S.; methodology, M.W.-K. and W.S.; software, M.W.-K.; formal analysis, W.S.; investigation, M.W.-K. and M.S.; resources, M.W.-K. and M.S.; data curation, M.W.-K. and M.S.; writing—original draft preparation, M.W.-K.; writing—review and editing, M.W.-K. and W.S.; supervision, W.S. All authors have read and agreed to the published version of the manuscript.

**Funding:** This research received no external funding.

**Data Availability Statement:** Data are contained within the article.

**Conflicts of Interest:** The authors declare no conflicts of interest.

## References

1. Sequeira, C.A.C.; Cardoso, D.S.P.; Martins, M.; Amaral, L. Novel materials for fuel cells operating on liquid fuels. *AIMS Energy* **2017**, *5*, 458–481. [[CrossRef](#)]
2. Bai, J.; Liu, D.; Yang, J.; Chen, Y. Nanocatalysts for Electrocatalytic Oxidation of Ethanol. *ChemSusChem* **2019**, *12*, 2117–2132. [[CrossRef](#)] [[PubMed](#)]
3. Lamy, C.; Belgsir, E.M.; Léger, J.M. Electrocatalytic oxidation of aliphatic alcohols: Application to the direct alcohol fuel cell (DAFC). *J. Appl. Electrochem.* **2001**, *31*, 799–809. [[CrossRef](#)]
4. Li, C.; Wang, K.; Xie, D. A review of approaches for the design of high-performance electrocatalysts for ethanol electrooxidation. *Surf. Interfaces* **2022**, *28*, 101594. [[CrossRef](#)]
5. Badwal, S.P.S.; Giddey, S.; Kulkarni, A.; Goel, J.; Basu, S. Direct ethanol fuel cells for transport and stationary applications—A comprehensive review. *Appl. Energy* **2015**, *145*, 80–103. [[CrossRef](#)]
6. Elsaïd, K.; Abdelfatah, S.; Abdel Elabsir, A.M.; Hassiba, R.J.; Ghouri, Z.K.; Vechot, L. Direct alcohol fuel cells: Assessment of the fuel's safety and health aspects. *Int. J. Hydrogen Energy* **2021**, *46*, 30658–30668. [[CrossRef](#)]
7. Sanchez, N.; Ruiz, R.; Hacker, V.; Cobo, M. Impact of bioethanol impurities on steam reforming for hydrogen production: A review. *Int. J. Hydrogen Energy* **2020**, *45*, 11923–11942. [[CrossRef](#)]
8. Ma, Y.; Ma, C.; Wang, Y.; Wang, K. Advanced Nickel-Based Catalysts for Urea Oxidation Reaction: Challenges and Developments. *Catalysts* **2022**, *12*, 337. [[CrossRef](#)]
9. Antolini, E.; Gonzalez, E.R. Alkaline direct alcohol fuel cells. *J. Power Sources* **2010**, *195*, 3431–3450. [[CrossRef](#)]
10. Rahim, M.A.A.; Hameed, R.M.A.; Khalil, M.W. Nickel as a catalyst for the electro-oxidation of methanol in alkaline medium. *J. Power Sources* **2004**, *134*, 160–169. [[CrossRef](#)]
11. Holade, Y.; Tuleushova, N.; Tingry, S.; Servat, K.; Napporn, T.W.; Guesmi, H.; Cornu, D.; Kokoh, K.B. Recent advances in the electrooxidation of biomass-based organic molecules for energy, chemicals and hydrogen production. *Catal. Sci. Technol.* **2020**, *10*, 3071–3112. [[CrossRef](#)]
12. Yuan, L.S.; Zheng, Y.X.; Jia, M.L.; Zhang, S.J.; Wang, X.L.; Peng, C. Nanoporous nickel-copper-phosphorus amorphous alloy film for methanol electro-oxidation in alkaline medium. *Electrochim. Acta* **2015**, *154*, 54–62. [[CrossRef](#)]
13. Mansor, M.; Timmiati, S.N.; Lim, K.L.; Wong, W.Y.; Kamarudin, S.K.; Nazirah Kamarudin, N.H. Recent progress of anode catalysts and their support materials for methanol electrooxidation reaction. *Int. J. Hydrogen Energy* **2019**, *44*, 14744–14769. [[CrossRef](#)]
14. Radenahmad, N.; Afif, A.; Petra, P.I.; Rahman, S.M.H.; Eriksson, S.G.; Azad, A.K. Proton-conducting electrolytes for direct methanol and direct urea fuel cells—A state-of-the-art review. *Renew. Sustain. Energy Rev.* **2016**, *57*, 1347–1358. [[CrossRef](#)]
15. Xu, C.; Wang, X.; Zhu, J. Graphene—Metal particle nanocomposites. *J. Phys. Chem. C* **2008**, *112*, 19841–19845. [[CrossRef](#)]
16. Das, S.; Dutta, K.; Shul, Y.G.; Kundu, P.P. Progress in Developments of Inorganic Nanocatalysts for Application in Direct Methanol Fuel Cells. *Crit. Rev. Solid State Mater. Sci.* **2015**, *40*, 316–357. [[CrossRef](#)]
17. Bong, S.; Kim, Y.-R.; Kim, I.; Woo, S.; Uhm, S.; Lee, J.; Kim, H. Graphene supported electrocatalysts for methanol oxidation. *Electrochem. Commun.* **2010**, *12*, 129–131. [[CrossRef](#)]
18. Askari, M.B.; Salarizadeh, P. Superior catalytic performance of NiCo<sub>2</sub>O<sub>4</sub> nanorods loaded rGO towards methanol electro-oxidation and hydrogen evolution reaction. *J. Mol. Liq.* **2019**, *291*, 111306. [[CrossRef](#)]
19. Noor, T.; Pervaiz, S.; Iqbal, N.; Nasir, H.; Zaman, N.; Sharif, M.; Pervaiz, E. Nanocomposites of NiO/CuO based MOF with rGO: An efficient and robust electrocatalyst for methanol oxidation reaction in DMFC. *Nanomaterials* **2020**, *10*, 1601. [[CrossRef](#)]
20. Urbańczyk, E.; Maciej, A.; Simka, W. Electrocatalytic properties of Co decorated graphene and graphene oxide for small organic molecules oxidation. *Int. J. Hydrogen Energy* **2020**, *45*, 1769–1783. [[CrossRef](#)]
21. Solmaz, R.; Döner, A.; Kardaş, G. Electrochemical deposition and characterization of NiCu coatings as cathode materials for hydrogen evolution reaction. *Electrochem. Commun.* **2008**, *10*, 1909–1911. [[CrossRef](#)]
22. Faid, A.Y.; Barnett, A.O.; Seland, F.; Sunde, S. NiCu mixed metal oxide catalyst for alkaline hydrogen evolution in anion exchange membrane water electrolysis. *Electrochim. Acta* **2021**, *371*, 137837. [[CrossRef](#)]
23. Zhang, L.; Zheng, Y.; Wang, J.; Geng, Y.; Zhang, B.; He, J.; Xue, J.; Frauenheim, T.; Li, M. Ni/Mo Bimetallic-Oxide-Derived Heterointerface-Rich Sulfide Nanosheets with Co-Doping for Efficient Alkaline Hydrogen Evolution by Boosting Volmer Reaction. *Small* **2021**, *17*, 2006730. [[CrossRef](#)] [[PubMed](#)]

24. Lu, X.; Yang, P.; Wan, Y.; Zhang, H.; Xu, H.; Xiao, L.; Li, R.; Li, Y.; Zhang, J.; An, M. Active site engineering toward atomically dispersed M–N–C catalysts for oxygen reduction reaction. *Coord. Chem. Rev.* **2023**, *495*, 215400. [[CrossRef](#)]
25. An, Y.; Ijaz, H.; Huang, M.; Qu, J.; Hu, S. The one-pot synthesis of CuNi nanoparticles with a Ni-rich surface for the electrocatalytic methanol oxidation reaction. *Dalton Trans.* **2020**, *49*, 1646–1651. [[CrossRef](#)]
26. Abutaleb, A. Electrochemical oxidation of urea on NiCu alloy nanoparticles decorated carbon nanofibers. *Catalysts* **2019**, *9*, 397. [[CrossRef](#)]
27. Hefnawy, M.A.; Fadlallah, S.A.; El-Sherif, R.M.; Medany, S.S. Synergistic effect of Cu-doped NiO for enhancing urea electrooxidation: Comparative electrochemical and DFT studies. *J. Alloys Compd.* **2022**, *896*, 162857. [[CrossRef](#)]
28. Zhang, L.; Wang, Y.; Liu, Z.; Yan, Z.; Zhu, L. Bimetallic nickel and copper supported Pt catalyst for ethanol electro-oxidation in alkaline solution. *Int. J. Electrochem. Sci.* **2018**, *13*, 2164–2174. [[CrossRef](#)]
29. Patel, D.A.; Giannakakis, G.; Yan, G.; Ngan, H.T.; Yu, P.; Hannagan, R.T.; Kress, P.L.; Shan, J.; Deshlahra, P.; Sautet, P.; et al. Mechanistic Insights into Nonoxidative Ethanol Dehydrogenation on NiCu Single-Atom Alloys. *ACS Catal.* **2023**, *13*, 4290–4303. [[CrossRef](#)]
30. De Waele, J.; Galvita, V.V.; Poelman, H.; Gabrovská, M.; Nikolova, D.; Damyanova, S.; Thybaut, J.W. Ethanol dehydrogenation over Cu catalysts promoted with Ni: Stability control. *Appl. Catal. A Gen.* **2020**, *591*, 117401. [[CrossRef](#)]
31. Jafarian, M.; Moghaddam, R.B.; Mahjani, M.G.; Gobal, F. Electro-catalytic oxidation of methanol on a Ni-Cu alloy in alkaline medium. *J. Appl. Electrochem.* **2006**, *36*, 913–918. [[CrossRef](#)]
32. Zheng, Y.; Qiao, J.; Yuan, J.; Shen, J.; Wang, A.-j.; Gong, P.; Weng, X.; Niu, L. Three-dimensional NiCu layered double hydroxide nanosheets array on carbon cloth for enhanced oxygen evolution. *Electrochim. Acta* **2018**, *282*, 735–742. [[CrossRef](#)]
33. Roy, A.; Talarposhti, M.R.; Normile, S.J.; Zenyuk, I.V.; De Andrade, V.; Artyushkova, K.; Serov, A.; Atanassov, P. Nickel-Copper Supported on Carbon Black Hydrogen Oxidation Catalyst Integrated into Anion-Exchange Membrane Fuel Cell. *Sustain. Energy Fuels* **2018**, *2*, 2268–2275. [[CrossRef](#)]
34. Zhao, X.; Fujii, M.; Shirai, T.; Watanabe, H.; Takahashi, M.; Zuo, Y. Electrocatalytic evolution of hydrogen on the NiCu/Al<sub>2</sub>O<sub>3</sub>/nanocarbon network composite electrode. *J. Mater. Sci.* **2011**, *46*, 4630–4637. [[CrossRef](#)]
35. Motlak, M.; Barakat, N.A.M.; El-Deen, A.G.; Hamza, A.M.; Obaid, M.; Yang, O.-B.; Akhtar, M.S.; Khalil, K.A. NiCu bimetallic nanoparticle-decorated graphene as novel and cost-effective counter electrode for dye-sensitized solar cells and electrocatalyst for methanol oxidation. *Appl. Catal. A Gen.* **2015**, *501*, 41–47. [[CrossRef](#)]
36. Shoeb, M.; Mobin, M.; Rauf, M.A.; Adnan, S.M.; Ansari, M.Y. Graphene nickel[sbnd]copper nanocomposite (Gr@NiCu NCs) as a binder free electrode for high energy density supercapacitor and antimicrobial application. *J. Mater.* **2021**, *7*, 815–827. [[CrossRef](#)]
37. Javan, H.; Asghari, E.; Ashassi-Sorkhabi, H. Design of new anodic bimetallic nanocatalyst composed of Ni–Cu supported by reduced carbon quantum dots for the methanol oxidation reaction. *Diam. Relat. Mater.* **2021**, *115*, 108348. [[CrossRef](#)]
38. Rana, S.; Jonnalagadda, S.B. A facile synthesis of Cu–Ni bimetallic nanoparticle supported organo functionalized graphene oxide as a catalyst for selective hydrogenation of p-nitrophenol and cinnamaldehyde. *RSC Adv.* **2017**, *7*, 2869–2879. [[CrossRef](#)]
39. Hou, C.; Zhang, M.; Halder, A.; Chi, Q. Graphene directed architecture of fine engineered nanostructures with electrochemical applications. *Electrochim. Acta* **2017**, *242*, 202–218. [[CrossRef](#)]
40. Vilana, J.; Gómez, E.; Vallés, E. Influence of the composition and crystalline phase of electrodeposited CoNi films in the preparation of CoNi oxidized surfaces as electrodes for urea electro-oxidation. *Appl. Surf. Sci.* **2016**, *360*, 816–825. [[CrossRef](#)]
41. Maniam, K.K.; Chetty, R.; Thimmappa, R.; Paul, S. Progress in the Development of Electrodeposited Catalysts for Direct Liquid Fuel Cell Applications. *Appl. Sci.* **2022**, *12*, 501. [[CrossRef](#)]
42. Wala, M.; Szcwcyk, M.; Leśniak–Ziółkowska, K.; Kazek–Kęsik, A.; Simka, W. Preparation of NiCuGO composite and investigation of its electrocatalytic properties in methanol oxidation. *Electrochim. Acta* **2022**, *425*, 140743. [[CrossRef](#)]
43. Wala, M.; Blacha–Grzechnik, A.; Stolarczyk, A.; Bajkacz, S.; Dydo, P.; Simka, W. Unexpected electrochemical oxidation of urea on a new NiCuGO composite catalyst. *Int. J. Hydrogen Energy* **2023**, *48*, 34229–34243. [[CrossRef](#)]
44. Barakat, N.A.M.; Motlak, M. CoxNiy-decorated graphene as novel, stable and super effective non-precious electro-catalyst for methanol oxidation. *Appl. Catal. B Environ.* **2014**, *154–155*, 221–231. [[CrossRef](#)]
45. Yang, J.; Shen, X.; Ji, Z.; Zhou, H.; Zhu, G.; Chen, K. In situ growth of hollow CuNi alloy nanoparticles on reduced graphene oxide nanosheets and their magnetic and catalytic properties. *Appl. Surf. Sci.* **2014**, *316*, 575–581. [[CrossRef](#)]
46. Glass, D.E.; Galvan, V.; Prakash, G.K.S. The Effect of Annealing Temperature on Nickel on Reduced Graphene Oxide Catalysts on Urea Electrooxidation. *Electrochim. Acta* **2017**, *253*, 489–497. [[CrossRef](#)]
47. Liu, X.; Liu, W.; Ko, M.; Park, M.; Kim, M.G.; Oh, P.; Chae, S.; Park, S.; Casimir, A.; Wu, G.; et al. Metal (Ni, Co)-Metal Oxides/Graphene Nanocomposites as Multifunctional Electrocatalysts. *Adv. Funct. Mater.* **2015**, *25*, 5799–5808. [[CrossRef](#)]
48. Duan, D.; Gao, J.; Wang, Y.; Zhou, X.; Liu, S.; Wang, Y. Electrodeposition of copper-cobalt bimetallic phosphide on nickel foam as an efficient catalyst for overall water splitting. *J. Electroanal. Chem.* **2023**, *939*, 117478. [[CrossRef](#)]
49. Sun, Q.; Li, Y.; Wang, J.; Cao, B.; Yu, Y.; Zhou, C.; Zhang, G.; Wang, Z.; Zhao, C. Pulsed electrodeposition of well-ordered nanoporous Cu-doped Ni arrays promotes high-efficiency overall hydrazine splitting. *J. Mater. Chem. A* **2020**, *8*, 21084–21093. [[CrossRef](#)]
50. Lotfi, N.; Shahrabi, T.; Yaghoobinezhad, Y.; Barati Darband, G. Electrodeposition of cedar leaf-like graphene Oxide@Ni–Cu@Ni foam electrode as a highly efficient and ultra-stable catalyst for hydrogen evolution reaction. *Electrochim. Acta* **2019**, *326*, 134949. [[CrossRef](#)]

51. Yan, W.; Wang, D.; Diaz, L.A.; Botte, G.G. Nickel nanowires as effective catalysts for urea electro-oxidation. *Electrochim. Acta* **2014**, *134*, 266–271. [[CrossRef](#)]
52. Plowman, B.J.; Jones, L.A.; Bhargava, S.K. Building with bubbles: The formation of high surface area honeycomb-like films via hydrogen bubble templated electrodeposition. *Chem. Commun.* **2015**, *51*, 4331–4346. [[CrossRef](#)] [[PubMed](#)]
53. Yang, S.B.; Tsai, Y.C.; Wu, M.S. Honeycomb-like copper/cuprous oxide with supported nickel hydroxide layer as an electrode material for electrochemical oxidation of urea. *J. Alloys Compd.* **2020**, *836*, 155533. [[CrossRef](#)]
54. Zhang, H.; Ye, Y.; Shen, R.; Ru, C.; Hu, Y. Effect of Bubble Behavior on the Morphology of Foamed Porous Copper Prepared via Electrodeposition. *J. Electrochem. Soc.* **2013**, *160*, D441–D445. [[CrossRef](#)]
55. Shin, H.C.; Liu, M. Copper foam structures with highly porous nanostructured walls. *Chem. Mater.* **2004**, *16*, 5460–5464. [[CrossRef](#)]
56. Li, R.; Li, Y.; Yang, P.; Ren, P.; Wang, D.; Lu, X.; Zhang, H.; Zhang, Z.; Yan, P.; Zhang, J.; et al. Key Roles of Interfacial OH<sup>-</sup> ion Distribution on Proton Coupled Electron Transfer Kinetics toward Urea Oxidation Reaction. *Small* **2023**, *19*, 2302151. [[CrossRef](#)] [[PubMed](#)]
57. Deng, Z.; Yi, Q.; Zhang, Y.; Nie, H. NiCo/C-N/CNT composite catalysts for electro-catalytic oxidation of methanol and ethanol. *J. Electroanal. Chem.* **2017**, *803*, 95–103. [[CrossRef](#)]
58. Miao, Z.; Xu, C.; Zhan, J.; Xu, Z. Morphology-control and template-free fabrication of bimetallic Cu–Ni alloy rods for ethanol electro-oxidation in alkaline media. *J. Alloys Compd.* **2021**, *855*, 157438. [[CrossRef](#)]
59. Nassif, N.; Ghayad, I.; Hamid, Z.A. Review article: Direct ethanol fuel cells as a renewable source of energy. *Egypt. J. Chem.* **2021**, *64*, 2723–2729. [[CrossRef](#)]
60. Martín-Yerga, D.; Henriksson, G.; Cornell, A. Insights on the ethanol oxidation reaction at electrodeposited PdNi catalysts under conditions of increased mass transport. *Int. J. Hydrogen Energy* **2021**, *46*, 1615–1626. [[CrossRef](#)]
61. Akhairi, M.A.F.; Kamarudin, S.K. Catalysts in direct ethanol fuel cell (DEFC): An overview. *Int. J. Hydrogen Energy* **2016**, *41*, 4214–4228. [[CrossRef](#)]
62. Almeida, C.V.S.; Tremiliosi-Filho, G.; Eguiluz, K.I.B.; Salazar-Banda, G.R. Improved ethanol electro-oxidation at Ni@Pd/C and Ni@PdRh/C core-shell catalysts. *J. Catal.* **2020**, *391*, 175–189. [[CrossRef](#)]
63. Altarawneh, R.M.; Brueckner, T.M.; Chen, B.; Pickup, P.G. Product distributions and efficiencies for ethanol oxidation at PtNi octahedra. *J. Power Sources* **2018**, *400*, 369–376. [[CrossRef](#)]
64. Guchhait, S.K.; Paul, S. Electrochemical development of Ni–Cu electrodes by direct and pulse current coating in ethanol electro-oxidation for DEFC. *Port. Electrochim. Acta* **2018**, *36*, 293–307. [[CrossRef](#)]
65. Rahmani, K.; Habibi, B. NiCo alloy nanoparticles electrodeposited on an electrochemically reduced nitrogen-doped graphene oxide/carbon-ceramic electrode: A low cost electrocatalyst towards methanol and ethanol oxidation. *RSC Adv.* **2019**, *9*, 34050–34064. [[CrossRef](#)] [[PubMed](#)]
66. Ghalkhani, M.; Mirzaie, R.A.; Banimostafa, A.; Sohoul, E.; Hashemi, E. Electrosynthesis of ternary nonprecious Ni, Cu, Fe oxide nanostructure as efficient electrocatalyst for ethanol electro-oxidation: Design strategy and electrochemical performance. *Int. J. Hydrogen Energy* **2023**, *48*, 21214–21223. [[CrossRef](#)]
67. Yu, J.; Ni, Y.; Zhai, M. Simple solution-combustion synthesis of Ni–NiO@C nanocomposites with highly electrocatalytic activity for methanol oxidation. *J. Phys. Chem. Solids* **2018**, *112*, 119–126. [[CrossRef](#)]
68. Cai, J.; Zeng, Y.; Guo, Y. Copper@palladium-copper core-shell nanospheres as a highly effective electrocatalyst for ethanol electro-oxidation in alkaline media. *J. Power Sources* **2014**, *270*, 257–261. [[CrossRef](#)]
69. Zheng, Y.; Wan, X.; Cheng, X.; Cheng, K.; Liu, Z.; Dai, Z. Advanced catalytic materials for ethanol oxidation in direct ethanol fuel cells. *Catalysts* **2020**, *10*, 166. [[CrossRef](#)]
70. Hassan, H.B.; Hamid, Z.A. Electrodeposited Ni–Cr<sub>2</sub>O<sub>3</sub> nanocomposite anodes for ethanol electrooxidation. *Int. J. Hydrogen Energy* **2011**, *36*, 5117–5127. [[CrossRef](#)]
71. Lycke, D.R.; Gyenge, E.L. Electrochemically assisted organosol method for Pt–Sn nanoparticle synthesis and in situ deposition on graphite felt support: Extended reaction zone anodes for direct ethanol fuel cells. *Electrochim. Acta* **2007**, *52*, 4287–4298. [[CrossRef](#)]
72. Bender, M.T.; Lam, Y.C.; Hammes-Schiffer, S.; Choi, K.S. Unraveling Two Pathways for Electrochemical Alcohol and Aldehyde Oxidation on NiOOH. *J. Am. Chem. Soc.* **2020**, *142*, 21538–21547. [[CrossRef](#)] [[PubMed](#)]
73. Kim, J.-W.; Park, S.-M. Electrochemical Oxidation of Ethanol at Nickel Hydroxide Electrodes in Alkaline Media Studied by Electrochemical Impedance Spectroscopy. *J. Korean Electrochem. Soc.* **2005**, *8*, 117–124. [[CrossRef](#)]
74. Chemchoub, S.; El Attar, A.; Oularbi, L.; Younsi, S.A.; Bentiss, F.; Jama, C.; El Rhazi, M. Electrosynthesis of eco-friendly electrocatalyst based nickel-copper bimetallic nanoparticles supported on poly-phenylenediamine with highest current density and early ethanol oxidation onset potential. *Int. J. Hydrogen Energy* **2022**, *47*, 39081–39096. [[CrossRef](#)]
75. Kamyabi, M.A.; Jadali, S. Rational design of PdCu nanoparticles supported on a templated Ni foam: The cooperation effect of morphology and composition for electrocatalytic oxidation of ethanol. *Int. J. Hydrogen Energy* **2021**, *46*, 39387–39403. [[CrossRef](#)]

**Disclaimer/Publisher’s Note:** The statements, opinions and data contained in all publications are solely those of the individual author(s) and contributor(s) and not of MDPI and/or the editor(s). MDPI and/or the editor(s) disclaim responsibility for any injury to people or property resulting from any ideas, methods, instructions or products referred to in the content.